

AN *EINSTEIN* X-RAY SURVEY OF OPTICALLY SELECTED GALAXIES. I. DATA

DAVID BURSTEIN

Department of Physics and Astronomy, Arizona State University, Tempe, AZ; burstein@samuri.la.asu.edu

C. JONES AND W. FORMAN

Harvard-Smithsonian Center for Astrophysics, Garden Street, Cambridge, MA 02138; cjf@cfa236.harvard.edu, wrf@cfa.harvard.edu

A. P. MARSTON

Department of Physics and Astronomy, Drake University, Des Moines, IA 50311; tm9991r@acad.drake.edu

AND

RONALD O. MARZKE

Harvard-Smithsonian Center for Astrophysics, Garden Street, Cambridge, MA 02138; and Dominion Astrophysical Observatory, Herzberg Institute of Astrophysics, National Research Council of Canada, 5071 West Saanich Road, Victoria, BC, Canada V8X 4M6; marzke@dao.nrc.ca

Received 1996 October 9; accepted 1997 January 17

ABSTRACT

We present the results of a complete *Einstein* imaging proportional counter X-ray survey of optically selected galaxies from the Shapley-Ames Catalog, the Uppsala General Catalogue, and the European Southern Observatory Catalog. Well-defined optical criteria are used to select the galaxies, and X-ray fluxes are measured at the optically defined positions. The result is a comprehensive list of X-ray detection and upper limit measurements for 1018 galaxies. Of these, 827 have either independent distance estimates or radial velocities. Associated optical, redshift, and distance data have been assembled for these galaxies, and their distances come from a combination of directly predicted distances and those predicted from the Faber-Burstein Great Attractor/Virgo-centric infall model.

The accuracy of the X-ray fluxes has been checked in three different ways; all are consistent with the derived X-ray fluxes being of ≤ 0.1 dex accuracy. In particular, there is agreement with previously published X-ray fluxes for galaxies in common with a 1991 study by Roberts et al. and a 1992 study by Fabbiano et al. The data presented here will be used in further studies to characterize the X-ray output of galaxies of various morphological types and thus to enable the determination of the major sources contributing to the X-ray emission from galaxies.

Subject headings: catalogs — galaxies: distances and redshifts — surveys — X-rays: galaxies

1. INTRODUCTION

Almost all X-ray surveys of galaxies published to date have used galaxy samples chosen on the basis of apparent optical brightness. These include the first surveys of the *HEAO 2* (*Einstein*) database (Long & Van Speybroeck 1981; Forman, Jones, & Tucker 1985; Fabbiano & Trinchieri 1987; Canizares, Fabbiano, & Trinchieri 1987 and references therein; Roberts et al. 1991), as well as the compilation by Fabbiano et al. (1992, hereafter F92). In total, 405 galaxies have *Einstein* measurements of X-ray properties studied in these surveys, all chosen from either the Shapley-Ames Catalog (Shapley & Ames 1932, hereafter S-A) or the Second Catalog of Bright Galaxies (de Vaucouleurs, de Vaucouleurs, & Corwin 1976, hereafter RC2). As analyzed by F92, 207 of these galaxies have 3σ X-ray detections.

However, consider the analogy with stars: the H-R diagram of the 100 brightest stars in the sky is very different from that of the 100 nearest stars. Is it possible that the same kinds of differences occur in galaxy samples similarly chosen, with the additional option that galaxies can be selected either by apparent brightness or by apparent size? A direct answer to this question is needed for a physical property of galaxies such as X-ray flux. The X-ray flux can come from several different sources within a given galaxy (e.g., hot thermal gas, accretion disks around binaries, central engines of active galaxies).

Given this motivation, the observational goal of the present survey was to obtain measurements of the X-ray

flux (or upper limits) at the positions of galaxies optically selected in two different ways, as viewed in the imaging proportional counter (IPC) fields obtained by the *Einstein* Observatory. One set, from the S-A catalog, is selected on the basis of apparent magnitude. Two data sets, one from the Uppsala General Catalogue (Nilson 1973, hereafter UGC) and European Southern Observatory Catalog (Lauberts 1982, hereafter ESO) are chosen on the basis of apparent size.

In the present paper, we present the X-ray measurements we made and the associated optical, redshift, and distance data for 1018 galaxies. A second paper will analyze the global properties of galaxies as found by this survey. Section 2 discusses how the galaxies were selected for study and how the X-ray data were obtained. In § 3 we discuss the origin of the non-X-ray data used for the galaxies in this survey: radial velocities, distances, magnitudes, and diameters. Many of the normal galaxies with published X-ray fluxes from *Einstein* fields have had their X-ray fluxes independently determined by this survey, in order to permit ready correspondence to previous results. Tests of the uniformity of the X-ray data are detailed in § 4, including a detailed comparison with the F92 published X-ray counts and fluxes. Section 5 gives a summary of the paper.

2. GALAXY SELECTION AND *EINSTEIN* X-RAY OBSERVATIONS

2.1. Combined Optical/X-Ray Selection of Galaxies

Most tests of the inclination dependence of the observed

properties of galaxies show that while the magnitudes of E and S0 galaxies are inclination-invariant, those of spiral galaxies are inclination-dependent (see Burstein, Haynes, & Faber 1991). This difference is due to the fact that spiral galaxies have visible dust distributed in their disks (see Giovanelli 1995), while the dust seen in E and S0 galaxies is well known to be localized near their centers. Specific tests on the UGC-measured and ESO-measured diameters of spiral galaxies indicate little change with inclination (e.g., Valentijn 1990; Burstein et al. 1991). However, interpreting these tests in terms of whether spiral galaxies actually have inclination-independent isophotal diameters is still in debate (cf. Davies, Jones, & Trewheila 1995; Burstein, Willick, & Courteau 1995; Giovanelli 1995).

Nevertheless, it is clear that the inclination dependencies of magnitudes and diameters for E/S0's is different from that for spiral and irregular galaxies. As such, it is not surprising that their relative numbers are different in a magnitude-limited sample (spirals undersampled) relative to a diameter-limited sample (spirals oversampled). One finds that galaxies of types E, S0, and S0/a comprise 24% of the S-A catalog (Sandage & Tammann 1981), while such galaxy types comprise only 16% of either the UGC or ESO catalogs. The present X-ray survey includes galaxies from all three catalogs, as one check for inclination-dependent selection effects influencing the results of X-ray studies of galaxies. Taken together, the data from all three catalogs comprises the most complete survey one can do for the brightest galaxies with the *Einstein* database.

The methodology we employ is to use the optical positions of galaxies to locate apertures of known size at the corresponding locations in the *Einstein* images and then to measure the observed count rate within these apertures, properly correcting for background count rate. As we expect to find upper limits to the fluxes of most galaxies, the need for accurate detection statistics make the use of relatively long exposures desirable. A lower exposure limit of 2000 s was chosen for images obtained with the IPC for UGC and ESO galaxies, and a lower limit of 1500 s was used for S-A galaxies (owing to the fact that the S-A galaxies are, in general, closer and generally of higher flux than the UGC and ESO galaxies). After some experimentation, high-resolution imager (HRI) exposures were not used for the final sample as the lower sensitivity of the HRI yielded much higher signal-to-noise upper limits, on average.

Galaxy selection for the present samples proceeded by cross-correlating the galaxy positions in each catalog with the positions of all *Einstein* IPC fields with at least the minimum exposure time. Each IPC pixel is 8" on a side; hence, galaxy positions accurate to $\approx 10''$ are sufficient for the purposes of this survey. Galaxies in the ESO and S-A catalogs have positions generally this accurate, and their quoted positions were used directly in the cross-correlation with IPC image positions.

Galaxies in the UGC have positions of mixed accuracy, some of which are very poor ($> 1'$). Improved positions for UGC galaxies were obtained in a two-step process: First, a cross-correlation was done between UGC-listed galaxy positions and IPC field positions. After further objective selection criteria were applied (common to all three catalogs and discussed below), a final list of 773 UGC galaxies was compiled. Second, accurate positions were either obtained from Dressel & Condon (1976) (320 of their 1800 galaxies are in our sample), or were measured by one of us (R. O. M.)

in the following manner: Transparent overlays were made of the field around the UGC position of each galaxy, to the scale of the Palomar Sky Survey (PSS) prints. Star positions and the UGC galaxy position were marked and the direction of north-south and east-west drawn. This overlay was then placed on the PSS print, and the position of the galaxy on the print, relative to the UGC position, was measured with a graduated reticle in both right ascension (R.A.) and declination (decl.). Comparison with 35 positions measured by Dressel & Condon indicate that the positions for 454 galaxies measured in this manner are accurate to $\pm 12''$, adequate for the purposes of this survey. A postsurvey recomparison with the UGC indicates that we missed at most 15 galaxies (for reasons such as bad search positions, IPC image not yet processed, etc.) that could otherwise have been in our survey. This omission has a negligible effect on the results of this survey.

Three optical selection criteria are applied to all three catalogs: galaxies with galactic reddening, $E(B-V) > 1.00$ (from Burstein & Heiles 1984 and unpublished data) were excluded, as well as galaxies without a listed morphological type. Galaxies with listed optical diameters larger than 5' are excluded from the UGC and ESO catalogs but not necessarily from the S-A catalog. Multiple galaxies listed in the UGC and ESO catalogs are included in this survey. X-ray selection criteria are discussed below.

The combination of optical and X-ray selection criteria results in 773 UGC galaxies in 483 IPC fields, 757 ESO galaxies in 232 IPC fields, and 404 S-A galaxies in 374 IPC fields. Of the 773 UGC galaxies, 103 are also in the S-A catalog; of the 757 ESO galaxies, 72 are in the S-A catalog. This survey therefore includes a total of 1759 galaxies with 2147 galaxy observations in 942 IPC fields (97 of these galaxies had X-ray counts measured by more than one of us independently). In addition, 194 measurements are taken at random positions in 8% of the IPC fields (see § 2.2).

2.2. X-Ray Flux Determinations

In obtaining the raw counts for the source and background regions from the IPC images, we used the energy range from 0.56 to 4.47 keV. Four box apertures are employed for measuring source counts, having sizes of 200", 232", 264", and 296" on a side. The size of the largest aperture was dictated by the necessity of uniformly measuring many galaxies in arbitrary positions on the IPC images.

The X-ray source and background counts on the IPC images were visually examined using the *HEAO* Image Processing monitor. Each IPC image was displayed and the position of each galaxy marked on the field. As with photoelectric aperture photometry of galaxies, in measuring background count rate, care was taken to avoid regions where the background was high, varying spatially, or where the IPC image was obstructed by the detector window support structure ("rib").

If the galaxy position lay close to a rib, or close to the edge of the field, the smaller apertures were measured if they could yield good data. However, in the majority of cases, placement near a rib or near the edge of the field meant that counts could not be measured for the galaxy. If the galaxy position lay within a region of diffuse emission (such as exists in a galaxy cluster), the galaxy was similarly excluded from X-ray measurement. Table 1 gives the numbers of galaxies rejected and the reasons for rejection. Background count rates were measured for each galaxy, both near the

TABLE 1
REASONS FOR EXCLUSION OF GALAXIES FROM X-RAY MEASUREMENTS

Catalog	On "Ribs"	Near Edge of IPC Field	In Diffuse Emission	In S-A Catalog	HRI Only	Image Not Usable
UGC.....	116	86	52	103	19	4
ESO	133	82	126	72	10	22
S-A ^a	27	16	33	...	4	...

^a Eleven galaxies in S-A sample also excluded for being too large for adequate coverage with survey apertures.

galaxy location and at "mirror-image" positions on the same field, after confirming that the background positions did not contain any obvious X-ray sources.

Two internal checks of our measuring procedure are made during the course of this survey. First, measurements are made at the positions of 194 "blank" fields, using the same procedures as for the sample galaxies. These fields are chosen in 73 IPC images that sample the range of exposure times used in this survey. The data for these blank fields are then processed in the same manner as for the galaxies. Second, because of the labor-intensive, interactive manner of deriving the aperture measurements, it is desirable that a subset of the galaxies be measured twice, once each by different "observers." The IPC emission of 97 galaxies were measured twice: once during the UGC/ESO phase of the program, and once later during the S-A phase. Comparison of the two sets of observations yield very close agreement. In order to preserve a similar signal-to-noise ratio, we do not average these two separate measurements of the same IPC image, but rather use just one.

X-ray fluxes are computed from the IPC images by correcting the net source counts in each aperture measured for the following explicit issues: (1) the exposure time, (2) the instrument dead time ($\sim 4\%$), (3) telescope vignetting (Harris et al. 1991), (4) H I column density, (5) spectral energy distribution of the source, and (6) predicted ratio of flux within measured aperture to total flux. The first three corrections are well known; for the vignetting corrections we assume a mean photon energy of 1.49 keV.

The next two corrections require knowledge of the H I column density (taken from Stark et al. 1992 and sources given in Marshall & Clark 1984) and the spectral energy distribution of the source. As the total number of counts for even the detected galaxies in our sample is generally too small to constrain the energy spectrum, we must assume a spectral energy distribution for these galaxies. As a test, we compare the differences in conversion rates that would arise from three different forms of the spectrum: (1) a 1 keV Raymond spectrum as appropriate for luminous ellipticals, (2) a 7 keV exponential spectrum as characteristic of binary X-ray sources, and (3) a power-law spectrum with a photon index of 1.5 typical of active galactic nuclei. For each kind of spectrum we generate the count rate to flux conversion for a range of H I values from 8×10^{19} to $3 \times 10^{21} N_H \text{ cm}^{-2}$. The hard exponential and power-law spectra give nearly the same count rate to flux conversions. The ratio of the 1 keV thermal conversion value to the other conversions ranges from 0.75 for low H I column density to 0.85 for high H I.

However, the X-ray emission mechanism for each galaxy, or even each type of galaxy, is not certain. For example, although binary sources are found in spiral galaxies, at least some spirals also have substantial diffuse emission. While

hot gas seems to dominate the X-ray emission from ellipticals, many X-ray-detected early-type galaxies contain active galaxy nuclei. Thus, at this stage in our analysis, we are reluctant to assign a particular spectrum to a particular class of galaxy and thereby bias the flux conversions. Instead, we choose to use an average count rate to flux conversions dependent only on the galactic H I column density, as given in Table 2 for all the galaxies in our samples, which is a compromise among the results from the three models.

The aperture-related correction is necessary as some galaxies could have fluxes determined only in smaller apertures. Smaller apertures are used when a source is near the edge of the field, near a rib, or near another source. Hence, data from all four X-ray apertures are used to examine the spatial distribution of the X-ray sources that are detected. Growth curves calculated from bright X-ray sources were used to extrapolate the flux from the largest aperture available for each galaxy observation, to a total flux. These corrections (listed in Table 4) are computed separately for elliptical galaxies, spiral galaxies, and central point source-dominated galaxies (such as Seyfert galaxies). Table 3 gives the number of galaxy observations for which each aperture was the largest measured. X-ray fluxes for 82% of the UGC galaxies with X-ray observations, 75% of the ESO galaxies, and 94% of the S-A galaxies are measured in the largest

TABLE 2
CONVERSION OF X-RAY COUNT RATE (1 IPC
count s^{-1}) TO 0.5–4.5 keV FLUX
($\text{ergs cm}^{-2} \text{s}^{-1} \times 10^{-11}$)

H I Column Density (10^{20})	X-Ray Correction Factor
30.0	5.376
20.06	4.718
13.41	4.280
8.963	3.977
5.992	3.752
4.006	3.571
2.678	3.420
1.790	3.293
1.197	3.188
0.800	3.103

TABLE 3
NUMBER OF GALAXIES FOR WHICH GIVEN
APERTURE IS THE LARGEST OBSERVED

Aperture	200"	232"	264"	296"
UGC.....	10	35	25	323
ESO	27	47	11	227
S-A.....	3	10	7	293

TABLE 4
CORRECTIONS TO APERTURE MEASUREMENTS USED TO ESTIMATE TOTAL X-RAY FLUXES

Source Type	200" Aperture Correction	232" Aperture Correction	264" Aperture Correction	296" Aperture Correction
Ellipticals/diffuse gas	1.44	1.27	1.16	1.07
Spirals	1.10	1.05	1.01	1.00 ^a
Point sources/Seyferts	1.08	1.05	1.03	1.01 ^a

^a The difference between spiral and point source arises from uncertainties; the difference is not significant.

aperture used in this survey (296" on a side). For those galaxies whose measured aperture is a smaller aperture, the observed flux in that smaller aperture is corrected to that of the largest aperture using the ratios in Table 4.

The signal-to-noise ratio is calculated in the usual manner assuming a Gaussian distribution of errors and taking into account both galaxy and background measurements. From our accuracy tests (see below), a signal-to-noise ratio (S/N) of 2.5 was chosen to distinguish between X-ray detections and nondetections in this sample. If a

galaxy has $S/N \geq 2.5$, the flux given is the flux observed. If a galaxy has $S/N < 2.5$, the flux given is $2.5 \times N$.

Finally, it should be clear that, although the selection of galaxies was done in an objective manner, only 5% of the sky is covered by IPC images. As many galaxies are IPC targets, the net effect is to incorporate a combination of several selection effects. We keep track of this effect by the size of the vignetting correction, which is close to unity for objects near the center of the *Einstein* IPC images. In the cases for galaxies observed on more than one IPC image, the vignetting correction value closest to unity is kept.

The number of galaxies included in this survey, relative to the total number of galaxies in the relevant optical catalogs, is shown in Figure 1. Galaxies are divided into four sections by morphological class: ellipticals and S0's, early-type spirals, late-type spirals and irregulars, and others (e.g., dwarfs, peculiars, multiple galaxies). This last category was used only for the UGC and ESO catalogs. Within each class, in Figure 1 we plot the fraction of galaxies included in the X-ray sample compared with those available from the whole catalog as a function of either apparent size (UGC and ESO) or apparent magnitude (S-A).

As is evident, the percentage of galaxies in the S-A sample with measured X-ray fluxes is an order of magnitude higher than in the diameter-selected sample. Yet, because of the order-of-magnitude-higher number of galaxies included in the UGC and ESO catalogs, the total number of galaxies with measured X-ray fluxes is comparable in each catalog. Within statistical fluctuations, the X-ray-observed samples are fair cross sections of both morphological types and apparent size (or magnitude) for these three catalogs.

3. OPTICAL, REDSHIFT, AND DISTANCE DATA

3.1. Optical Data

Optical diameters, magnitudes, and axial ratios for blue magnitude data are given for each galaxy in this survey when available. The primary source for the S-A sample is the RC2, for which apparent magnitudes (either on the Harvard corrected system or on the BT system) are given, together with isophotal diameters (to the 25th magnitude isophote) and axial ratios. UGC galaxies have optical data obtained primarily from the UGC, for which diameters, axial ratios, and magnitudes are listed. UGC galaxy magnitudes that are 15.7 or brighter come from the Zwicky et al. (1961–1968) catalog. Zwicky magnitudes require correction to be placed on a common system in reasonable accord with the RC2 system. The correction procedure adopted here is that advocated by Huchra (1976).

ESO galaxies have optical data obtained from the more recent photographic surface photometry published by Lauberts & Valentijn (1989). This photometry is available for 85% of the original 16,154 galaxies in the ESO survey

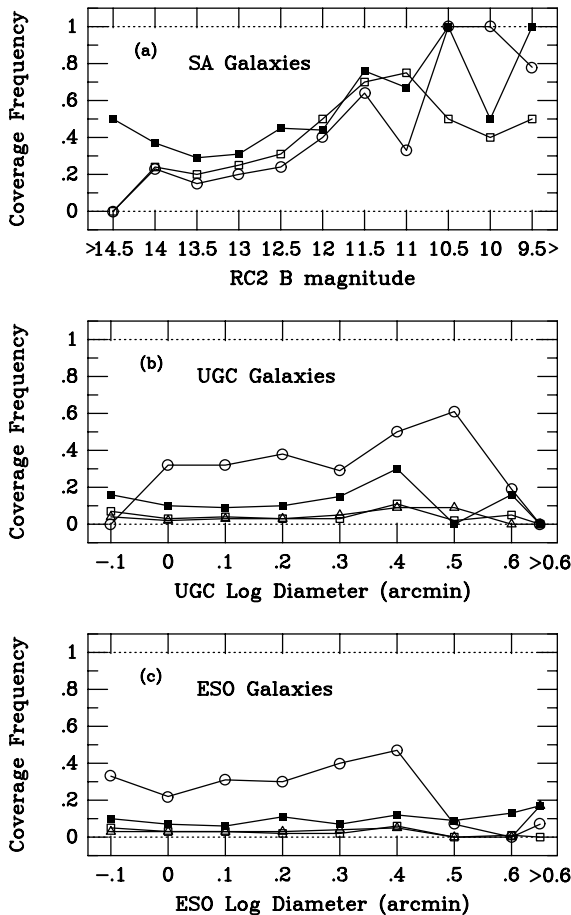


FIG. 1.—The fraction of galaxies surveyed in each of the three catalogs used for this survey: (a) Shapley-Ames (SA), (b) Uppsala General Catalogue (UGC), and (c) European Southern Catalog (ESO). In each case, the galaxies are divided by Hubble types: E+S0+S0/a galaxies (filled squares), early-type spiral galaxies (open circles), late-type spirals + irregulars (open squares), and multiple/double/peculiar galaxies (open triangles; only in panels b and c). The fraction of galaxies in our survey in the S-A catalog are plotted as a function of apparent magnitude. For both the UGC and ESO catalogs, they are plotted as a function of log diameter in arcminutes.

and, as such, is available for a similar percentage of the galaxies in the present survey. The 25th blue magnitude isophotal diameters and total blue magnitudes used here are taken from Lauberts & Valentijn; axial ratios are taken from the original ESO catalog (Lauberts 1982).

Galactic reddenings, $E(B-V)$ are taken from Burstein & Heiles (1984) for the RC2 and UGC galaxies and separately calculated using the Burstein-Heiles reddening maps for ESO galaxies. The reddenings are expressed in terms of Burstein-Heiles-defined galactic extinction, $A_B = 4 \times E(B-V)$. Redshift-dependent K -corrections are calculated using the precepts of the RC2.

3.2. Redshifts and Distances

Heliocentric radial velocities are obtained primarily from the computer-readable version of the Third Reference Catalog of Bright Galaxies (de Vaucouleurs et al. 1991, hereafter RC3), as distributed by H. G. Corwin, Jr. These values are then supplemented by examination of the NASA Extragalactic Database (NED), as of 1996 February.

Distances for galaxies are determined in a two-step process. First, all the galaxies in this sample are cross-correlated with the galaxies in the Mark III Catalog of Galaxy Peculiar Velocities (Willick et al. 1995, 1996a, 1996b; references cited in notes to Tables 12, 13, and 14). We use the distances termed "inhomogeneous Malmquist-corrected" as given in the Mark III. Distances of galaxies are expressed in km s^{-1} units, using $H_0 = 75 \text{ km s}^{-1} \text{ Mpc}^{-1}$. Galaxies without directly measured distances but with measured radial velocities have their distances calcu-

lated, in terms of km s^{-1} , by the Great Attractor velocity field model of Faber & Burstein (1988).

3.3. The Observed and Derived Data Sets

Tables 5, 6, and 7 contain the observed data for this survey for the galaxies in the UGC, ESO, and S-A catalogs, respectively. Only those galaxies with X-ray measurements are included. This includes 313 S-A galaxies, 393 UGC (not S-A) galaxies, and 312 ESO (not S-A) galaxies, for a total of 1018 galaxies with X-ray observations. These have the following format: Column (1) gives the name of the galaxy; column (2) the apparent blue magnitude of the galaxy; column (3) the logarithm of the blue isophotal diameter; column (4) the morphological type number, T (as explained in the notes to Tables 5, 6, and 7). Column (5) gives the *Einstein* field number used for the X-ray data. A value of -1 indicates that multiple fields were used (see Table 8 for a listing of these fields). Column (6) gives the total exposure time for this galaxy (including all IPC images sampled). Columns (7) and (8) give the R.A. (1950) and decl. (1950) position at which the X-ray image was searched. Column (9) gives the X-ray count rate measured for this galaxy, in units of 1000 times the observed count rate. This count rate is corrected only for background and dead-time correction. Column (10) gives the error on this count rate, in the same units. The values in column (11) are the multiplicative IPC count rate to flux conversion for the energy range from 0.5 to 4.5 keV for an IPC count rate of 1 count s^{-1} and an X-ray spectrum, as discussed in section § 2.2. Column (12) contains the IPC vignetting correction. If more than one

TABLE 5
PROPERTIES OF SHAPLEY-AMES GALAXIES WITH X-RAY OBSERVATIONS

Name (1)	B_T (2)	$\log D$ 0.1 (3)	Type (4)	IPC Field (5)	Exposure (s) (6)	R.A. (1950) (7)	Decl. (1950) (8)	X-Ray Count Rate (9)	X-Ray Sigma (10)	Conversion (11)	Vignette Correction (12)	Aperture (13)
N128	12.60	1.53	-2	6643	1646	0 26.68	2 35.3	3.35	2.58	3.432	0.996	4
N221	9.15	1.88	-6	573	21155	0 39.97	40 35.5	7.23	0.92	3.794	0.577	4
N227	12.78	1.32	-5	5393	9834	0 40.06	-1 48.3	0.89	0.65	3.443	0.489	1
SMC	2.79	3.45	9	-1	22219	0 51.00	-73 06.0	6.50	2.78	3.771	0.960	4
N309	12.40	1.49	5	8992	5201	0 54.19	-10 11.1	3.14	1.47	3.531	0.836	4
I1613	9.99	2.08	10	2086	7110	1 02.22	1 51.0	1.60	1.40	3.439	0.996	4
N521	12.50	1.53	4	153	1087	1 21.99	1 28.3	-4.90	2.05	3.477	0.799	4
N520	12.05	1.68	-7	2088	4669	1 22.00	3 31.9	3.05	1.66	3.479	0.996	4
N524	11.50	1.51	-1	2089	5948	1 22.17	9 16.7	12.93	1.93	3.656	0.992	4
N533	12.50	1.57	-5	153	1087	1 22.95	1 30.0	29.44	5.65	3.477	0.496	2
N578	11.50	1.68	5	424	2743	1 28.09	-22 55.5	2.99	2.16	3.175	0.996	4
N596	11.78	1.54	-5	7951	9782	1 30.36	-7 17.3	1.06	1.05	3.484	0.841	4
N598	6.26	2.79	6	2096	20531	1 31.05	30 23.9	321.62	4.11	3.140	0.992	4
N613	10.79	1.76	4	3556	2033	1 31.98	-29 40.3	1.75	1.64	3.269	0.654	1
N615	12.30	1.60	3	7951	9782	1 32.59	-7 35.8	-0.11	0.90	3.484	0.498	4
N625	12.21	1.48	9	5257	1758	1 32.90	-41 41.0	3.07	2.71	3.269	0.994	4
N628	9.75	2.01	5	7042	6867	1 34.01	15 31.6	5.88	1.45	3.639	0.996	4
N672	11.35	1.82	6	7756	6311	1 45.09	27 11.1	0.61	1.31	3.846	0.948	4
N720	11.15	1.64	-5	5769	4628	1 50.57	-13 59.1	24.25	2.78	3.228	0.996	4
N772	11.10	1.85	3	464	889	1 56.59	18 46.0	7.49	4.43	3.767	0.995	4
N877	12.50	1.37	4	6339	5586	2 15.27	14 18.9	5.87	1.50	3.898	0.839	4
N936	11.10	1.72	-1	5771	5824	2 25.08	-1 22.7	8.20	1.72	3.417	0.992	4
N941	13.00	1.45	5	5118	6637	2 25.92	-1 22.5	2.96	1.38	3.419	0.907	4

NOTE.—Table 5 is published in its entirety in computer-readable form in the AAS CD-ROM Series, Vol. 9. Col. (1): Galaxy name (N = NGC, I = IC). Col. (2): Observed blue apparent magnitude, B_T , taken from RC2. Col. (3): Observed RC2 diameter, expressed as $\log D$ (0.1). Col. (4): Hubble numerical type. Type numbers as with RC2 numbering system (e.g., $-5 = E$, $0 = S0/a$, $5 = Sc$, $10 = Im$), but with the addition that 10 galaxies have the numerical type -7 . Col. (5): IPC field number (-1 if multiple IPC fields are used; see Table 8). Col. (6): Exposure time used (s). Cols. (7) and (8): Epoch 1950 R.A. and decl. position searched on the IPC image(s). Cols. (9) and (10): X-ray count rate and error, in units of 1000 times observed count rate, only dead-time-corrected and background-corrected. Col. (11): Multiplicative correction factor for H I column density and source energy distribution, to transform vignetting-corrected and dead-time-corrected source counts to flux in units of $10^{-11} \text{ ergs cm}^{-2} \text{ s}^{-1}$. Col. (12): Vignetting correction, to be divided into observed count rate. Col. (13): Numerical code for the largest aperture used to obtain the X-ray count rate. 1 = 200" aperture, 2 = 232" aperture, 3 = 264" aperture, and 4 = 296" aperture.

TABLE 6
PROPERTIES OF UGC GALAXIES WITH X-RAY OBSERVATIONS

Name (1)	m_B (2)	log D 0.1 (3)	Type (4)	IPC Field (5)	Exposure (s) (6)	R.A. (1950) (7)	Decl. (1950) (8)	X-Ray Count Rate (9)	X-Ray Sigma (10)	Conversion (11)	Vignette Correction (12)	Aperture (13)
U81	15.70	1.15	14	6718	2566	0 06.50	10 38.8	-0.27	1.14	3.739	0.629	2
U144	15.70	1.00	15	10431	10445	0 12.85	15 57.5	2.20	1.02	3.582	0.596	4
U204	14.60	1.15	16	7765	7970	0 18.68	22 48.9	-0.73	0.98	3.568	0.501	4
U305	15.30	1.15	16	5417	2278	0 28.02	13 04.9	-0.16	1.18	3.626	0.656	2
U387	13.80	1.32	1	-1	9521	0 35.82	29 14.0	2.72	1.59	3.666	0.871	4
U412	15.50	1.00	11	7917	4477	0 36.82	29 29.4	-1.37	0.76	3.663	0.474	2
U442	15.40	1.26	16	6828	11867	0 39.15	32 43.3	0.76	0.95	3.734	0.770	4
U446	17.00	1.08	20	6828	11867	0 39.56	32 56.1	-2.03	0.90	3.734	0.744	4
U499	15.00	1.20	10	2660	2108	0 46.07	31 40.9	13.66	3.31	3.737	0.988	4
U509	16.50	1.15	16	2660	2108	0 47.07	31 19.6	1.35	2.01	3.737	0.556	4
U524	14.50	0.95	14	5123	7090	0 48.88	29 07.1	74.73	3.84	3.733	0.502	4
U573	14.00	1.15	70	5988	2896	0 53.43	23 51.0	2.00	1.98	3.581	0.777	4
U595	14.80	1.15	50	-1	10569	0 55.01	-0 22.4	0.51	1.76	3.476	0.531	4
U611	14.50	1.04	70	3995	2528	0 56.25	0 19.0	-0.73	1.32	3.476	0.493	2
U626	15.00	1.00	16	3995	2528	0 58.12	-0 00.1	-0.51	1.46	3.476	0.573	4
U633	14.60	1.23	14	2619	2181	0 58.61	31 14.2	2.02	2.00	3.712	0.529	4
U657	17.00	1.08	31	1759	12080	1 01.23	32 41.9	-0.09	0.83	3.699	0.700	4
U711	14.80	1.60	16	2011	2934	1 06.05	1 22.5	0.93	1.56	3.451	0.868	3
U712	14.50	1.08	12	6308	6470	1 06.22	32 22.1	0.13	0.85	3.712	0.573	2
U714	14.50	1.11	16	6308	6470	1 06.47	31 52.7	-1.84	1.03	3.712	0.500	4
U768	15.40	1.08	50	8458	6053	1 10.58	2 01.6	3.24	1.33	3.468	0.720	4
U784	15.00	1.18	14	5394	14433	1 11.52	-2 00.4	0.01	0.63	3.595	0.565	4

NOTE.—Table 6 is published in its entirety in computer-readable form in the AAS CD-ROM Series, Vol. 9. Col. (1): UGC galaxy name. Col. (2): Observed blue apparent magnitude, m_B , taken from Zwicky et al. (1961–1968) for $m_B < 15.7$; from Nilson (1973) estimate otherwise. Col. (3): Observed UGC diameter, expressed as log D (0.1), consistent with RC2 definition. Col. (4): Hubble numerical type. Type numbers for UGC and ESO galaxies have been defined by Burstein in the following manner: E, E/S0 = 1; S0 = 10; S0/a = 11; Sa = 12; Sa/b = 13; Sb = 14; Sb/c = 15; Sc = 16; Sc/Sd = 17; Sd = 18; Sd/Irr = 19; Irr = 20; “S,” no subtype = 30; “I,” no subtype = 31; “S0,” no subtype = 35; dwarf galaxy = 40; compact galaxy = 50 or 51; double or multiple galaxies, galaxy groups or galaxy clusters = 60–65; peculiar galaxies = 70; no classification given = 90. Class 60 is needed because in both the UGC and ESO catalogs a single entry might be a multiple system. Col. (5): IPC field number (–1 if multiple IPC fields are used; see Table 8). Col. (6): Exposure time used (s). Cols. (7) and (8): Epoch 1950 R.A. and decl. position searched on the IPC image(s). Cols. (9) and (10): X-ray count rate and error, in units of 1000 times observed count rate, only dead-time-corrected and background-corrected. Col. (11): Multiplicative correction factor for H I column density and source energy distribution, to transform vignetting-corrected and dead-time-corrected source counts to flux in units of 10^{-11} ergs cm^{-2} s^{-1} . Col. (12): Vignetting correction, to be divided into observed count rate. Col. (13): Numerical code for the largest aperture used to obtain the X-ray count rate. 1 = 200" aperture, 2 = 232" aperture, 3 = 264" aperture, and 4 = 296" aperture.

IPC image is used for the observed count rate, the vignetting correction given here is the exposure-weighted average of the individual vignetting corrections. Column (13) indicates which of the four apertures were used to obtain the observed count rate (1 = smallest, 4 = largest).

Tables 9, 10, and 11 list those galaxies included in the original survey but for which X-ray measurements were not made. The reasons for exclusion (discussed in more detail previously in § 2.2) include obscuration by the ribs of the IPC, near or off the edge of the IPC image, only in HRI images, or within diffuse X-ray emission. Eleven S-A galaxies that were too large for the apertures used in this survey also were not observed. In Tables 9, 10, and 11, column (1) has the name of the galaxy, column (2) the apparent blue magnitude of the galaxy (if available), and column (3) the numerical code indicating the reason for omission (see notes to the tables for an explanation of this code.)

Tables 12, 13, and 14 contain the distance-dependent derived parameters for the X-ray measured galaxies in this survey. Column (1) gives the galaxy name, column (2) the heliocentric radial velocity. Column (3) gives the distance used for this galaxy, in units of Mpc (assuming $H_0 = 75$ km s^{-1} Mpc $^{-1}$), while column (4) gives a numerical code for the source of this distance, as detailed in the table notes. Columns (5), (6), and (7) give the absolute B magnitude, log of galaxy diameter (in kpc), and fully corrected absolute X-ray luminosity for this galaxy. Column (8) notes which

galaxies are generally classified as Seyfert galaxies. Tables 12, 13, and 14 include 329 UGC galaxies, 180 ESO galaxies, and all 313 S-A galaxies, for a total of 822 galaxies (81% of the total sample) with both X-ray observations and known distances. The 196 galaxies in the UGC and ESO samples that have measured X-ray fluxes (both detected and upper limits) but do not yet have radial velocity measurements are given in Table 15. Included among these are 11 galaxies whose X-ray emission was detected with *Einstein*.

4. INTERNAL AND EXTERNAL ESTIMATES OF THE ACCURACY OF THE X-RAY DATA

4.1. Sky Measurements and “Blank” Fields

For 251 of the 1018 galaxies with X-ray measurements (24.7%), the observed X-ray flux has an S/N of 2.5 or better and a redshift is known. Correcting this percentage for the number of false detections, which we determined through a similar analysis of blank fields, we have a detection rate of 22.6%. Most of the galaxies in this survey have only X-ray upper limit values. The fact that most galaxies in this survey would not be detected at a significant level was expected at the outset. Indeed, one of the principal aims of this survey was to assemble enough galaxies in each morphological class so that an average X-ray flux per class could be derived, even if most individual galaxies were not detected. Given this intent, it was important to be able to verify the statistical accuracy of noise estimates.

TABLE 7
PROPERTIES OF ESO GALAXIES WITH X-RAY OBSERVATIONS

Name (1)	m_B (2)	$\log D$ 0.1 (3)	Type (4)	IPC Field (5)	Exposure (s) (6)	R.A. (1950) (7)	Decl. (1950) (8)	X-Ray Count Rate (9)	X-Ray Sigma (10)	Conversion (11)	Vignette Correction (12)	Aperture (13)
E349-G31.....	15.54	0.91	20	4517	4342	0 05.68	-34 51.4	0.56	1.36	3.175	0.509	4
E349-G37.....	15.04	0.97	30	4518	3158	0 08.43	-35 29.3	-0.09	1.36	3.181	0.416	4
E50-G10.....	16.43	1.15	16	-1	18842	0 22.27	-72 01.6	0.32	1.47	3.530	0.878	4
E474-G05.....	14.66	1.33	19	8989	2191	0 34.75	-22 51.6	0.37	2.17	3.232	0.933	4
E540-G19.....	14.83	0.94	14	5766	10614	0 43.48	-20 52.9	0.32	0.96	3.240	0.705	4
E540-G24.....	15.70	0.80	15	5766	10614	0 45.13	-20 45.5	-0.11	0.69	3.240	0.725	2
E540-G26.....	15.75	0.71	30	5766	10614	0 45.15	-20 57.5	-0.36	1.05	3.240	0.907	4
E540-G25.....	14.69	1.00	14	5766	10614	0 45.15	-20 47.5	-0.87	0.87	3.240	0.762	4
E29-G26.....	0.00	-1.10	30	-1	5819	0 58.02	-74 52.9	-1.55	1.54	3.624	0.545	4
E541-G16.....	16.23	1.05	14	2333	4465	1 01.55	-21 38.4	-0.73	0.88	3.251	0.430	2
E244-G01.....	16.06	1.01	13	6088	5660	1 10.12	-46 09.3	-0.82	1.06	3.326	0.557	4
E113-IG45.....	14.08	0.89	30	523	2674	1 21.85	-59 03.9	1415.07	23.62	3.404	0.994	4
E476-G14.....	15.22	1.01	30	424	2743	1 27.28	-22 34.8	-0.17	1.03	3.175	0.602	1
E29-G47.....	0.00	-1.10	30	7991	11892	1 33.25	-73 52.1	-0.53	0.76	3.699	0.540	4
E543-G03.....	0.00	-1.10	30	905	5301	1 35.45	-18 14.9	-1.20	1.31	3.225	0.806	4
E546-G29.....	16.12	0.93	14	3996	3787	1 35.52	-24 37.3	-1.85	1.46	3.190	0.892	4
E543-G06.....	0.00	-1.10	10	-1	17526	1 36.25	-18 05.2	-0.08	1.43	3.225	0.905	4
E543-G09.....	0.00	-1.10	30	6953	5301	1 37.05	-17 53.2	-0.75	1.16	3.225	0.646	4
E413-G25.....	16.74	0.82	30	3719	9620	1 40.48	-30 36.5	1.68	1.25	3.276	0.970	4
E114-G16.....	13.89	1.23	12	846	2826	1 56.28	-61 27.3	1.10	1.18	3.464	0.627	1
E298-G07.....	14.80	1.05	16	5388	4433	2 04.12	-37 34.2	-0.80	1.22	3.246	0.536	4
E298-G10.....	15.55	1.02	13	5388	4433	2 06.32	-38 21.7	0.50	1.43	3.246	0.511	4
E298-G11.....	15.00	0.94	14	4253	6133	2 06.65	-40 22.0	-0.91	0.75	3.247	0.459	2

NOTE.—Table 7 is published in its entirety in computer-readable form in the AAS CD-ROM Series, Vol. 9. Col. (1): ESO catalog name for galaxy. Col. (2): Observed blue apparent magnitude, m_B , taken from Lauberts & Valentijn (1989). 0.00 means no magnitude available. Col. (3): Observed ESO diameter from Lauberts & Valentijn (1989), measured at the $B = 25$ th mag isophote, to be consistent with the RC2 diameter, expressed as $\log D(0.1)$. -1.10 means no diameter available. Col. (4): Hubble numerical type. Type numbers for UGC and ESO galaxies have been defined by Burstein in the following manner: E, E/S0 = 1; S0 = 10; S0/a = 11; Sa = 12; Sa/b = 13; Sb = 14; Sb/c = 15; Sc = 16; Sc/Sd = 17; Sd = 18; Sd/Irr = 19; Irr = 20; "S," no subtype = 30; "I," no subtype = 31; "SO," no subtype = 35; dwarf galaxy = 40; compact galaxy = 50 or 51; double or multiple galaxies, galaxy groups or galaxy clusters = 60–65; peculiar galaxies = 70; no classification given = 90. Class 60 is needed as in both the UGC and ESO catalogs a single entry might be a multiple system. Col. (5): IPC field number (-1 if multiple IPC fields are used; see Table 8). Col. (6): Exposure time used (s). Cols. (7) and (8): Epoch 1950 R.A. and decl. position searched on the IPC image(s). Cols. (9) and (10): X-ray count rate and error, in units of 1000 times observed count rate, only dead-time-corrected and background-corrected. Col. (11): Multiplicative correction factor for H I column density and source energy distribution, to transform vignetting-corrected and dead-time-corrected source counts to flux in units of 10^{-11} ergs cm^{-2} s^{-1} . Col. (12): Vignetting correction, to be divided into observed count rate. Col. (13): Numerical code for the largest aperture used to obtain the X-ray count rate. 1 = 200" aperture, 2 = 232" aperture, 3 = 264" aperture, and 4 = 296" aperture.

This was done in two ways. First, the 194 blank fields were measured. As noted above, these were treated in the same way as the galaxy measurements. S/N histograms from the blank field observations were compared with those formed from the program galaxies. Second, comparisons were made among the 97 galaxies that were twice measured independently.

Figure 2 shows the histogram of the S/N measurements of the blank field measurements. Also plotted in this histogram is the expected Gaussian distribution of S/N. There is a slight tendency for the blank fields to show a small net positive S/N (+0.095) compared with a Gaussian distribution. Nevertheless, the measurement of these blank fields is not expected to produce a Gaussian distribution based at S/N = 0 but, rather, to be representative of what we would have measured in the absence of X-ray flux at these galaxy positions.

In Figures 3 and 4 we show X-ray measurement signal-to-noise distributions for E/S0 galaxies (Fig. 3) and spiral and irregular galaxies (Fig. 4) separately for the three catalog samples and for all the data together. Plotted over these histogram distributions is the measured distribution for the blank fields, scaled to match the number of galaxies actually measured in each sample. It is satisfying that the negative S/N tail of the blank fields defines the minimum S/N of all of the galaxy samples in which most galaxies are

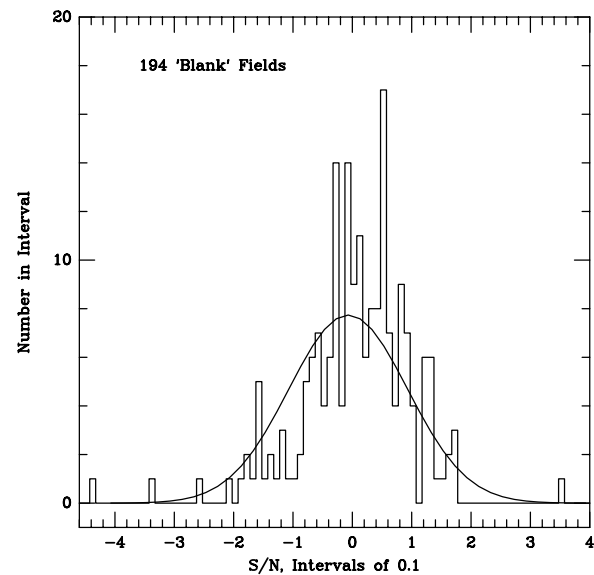


FIG. 2.—The distribution of calculated IPC S/N of the 194 "blank" fields, randomly selected as being free of obvious X-ray emission on the program IPC fields and reduced in the same manner as the program measurements. The distribution is very close to being Gaussian, with a small net offset of 0.095 in S/N.

TABLE 8
OBJECTS FOR WHICH MULTIPLE IPC
OBSERVATIONS WERE USED

Name	IPC Field
S-A Galaxies	
SMC	593, 6755, 7988
N1317	1883, 1884, 10571
N1389	4128, 4129
N2992	3060, 3061, 6376
N4038	469, 7054
N4192	6978, 6979
N4303	3267, 6986
N4382	2121, 6994
N4654	7013, 7014
N4754	7024, 7025
N5128	477, 4493
N6503	2720, 8846
N7469	1977, 1978
N1068	1927, 1928
N1365	3058, 3059
N1398	2096, 2097
N3430	3936, 6675
N4178	4055, 6976, 6977
N4260	2672, 6309
N4321	4300, 4301
N4569	4045, 4314
N4665	7016, 7017
N4762	7024, 7025
N5898	1998, 9647
N6946	422, 10314, 10597
N7582	3066, 3067, 6385
N1316	1883, 1884, 10571
N1387	4128, 4129
N1566	1937, 1938
N3516	1947, 1948
N4190	7816, 7817
N4261	2672, 6309
N4365	6992, 6993
N4639	7013, 7014
N4698	7022, 7023
N5068	5807, 8996
N6300	4952, 6373
N7213	2236, 6714
N7590	3066, 3067, 6218
UGC Galaxies	
U387	7697, 7917
U3087	350, 351
U7227	6978, 6979
U7344	2715, 6712
U7465	6992, 6993
U7784	4045, 4314
U7915	7013, 7014
U8971	7769, 9021
U9822	461, 2604
U10512	2060, 5694
U11130	5689, 9420
U12641	6972, 6973
U595	1770, 1771
U3902	211, 838
U7240	6978, 6979
U7359	2672, 6309
U7472	6992, 6993
U7855	2129, 2130
U8672	7203, 10548
U9176	2143, 6685
U10015	240, 6069
U10599	5210, 5211
U12231	7362, 7363, 7364
U2874	7814, 7815
U7173	352, 3453
U7269	6978, 6979
U7372	2672, 6309
U7492	6992, 6993

TABLE 8—Continued

Name	IPC Field
U7863	2129, 2130
U8956	7769, 9021
U9469	494, 2690
U10336	322, 7695
U10684	2062, 4208, 5688, 5716
U12324	1977, 1978
ESO Galaxies	
E50-G10	602, 4969
E301-G08	1883, 1884, 10571
E492-G07	3125, 5091, 5093
E514-G03	1998, 9647
E29-G26	9044, 9968
E357-G24	1884, 10571
E322-G62	6055, 6056
E466-G23	5201, 5202
E543-G06	905, 6952, 6953
E155-G26	1827, 4254
E514-G01	1998, 7493, 9647
E466-G32	5201, 5202

not detected. This is particularly true for spiral and irregular galaxies and gives us confidence in the accuracy of our measurements.

The histograms in Figures 3 and 4 show two trends. First, it is obvious that almost all the S-A galaxies have detected X-ray flux at some level. In contrast, for most of the non-S-A UGC and ESO galaxies, the measured X-ray fluxes are clearly upper limits. Second, in each catalog it is

TABLE 9
SHAPLEY-AMES GALAXIES WITHOUT
X-RAY OBSERVATIONS

Name (1)	B_T (2)	Omit (3)
N205	8.85	7
N253	8.04	7
N1055	11.40	3
N1297	12.61	2
N1425	11.60	2
N1549	10.87	2
N2911	12.60	4
N2993	13.10	4
N3031	7.75	7
N3226	12.30	4
N3309	12.90	4
N3607	10.95	4
N3687	12.85	3
N3982	11.91	2
N4214	10.20	2
N4270	13.10	2
N4417	12.00	4
N4472	9.31	4

NOTE.—Tables 9, 10, and 11 are published in their entirety in computer-readable form in the AAS CD-ROM Series, Vol. 9. For Table 9 alone, col. (1): Galaxy name; N = NGC, I = IC. (2): Observed blue apparent magnitude, B_T , taken from the RC2. For Tables 9, 10, and 11, col. (3): Reason for omission: 0 = image not available in processed form; 2 = on IPC “ribs”; 3 = on or off edge of IPC field; 4 = in obvious diffuse emission; 7 = too large for this survey; 9 = only HRI image available.

TABLE 10
UGC GALAXIES WITHOUT X-RAY
OBSERVATIONS

Name (1)	m_B (2)	Omit (3)
U180	15.30	4
U253	15.30	3
U443	15.50	2
U479	15.30	3
U508	12.60	2
U540	14.10	2
U598	14.40	3
U682	13.90	4
U687	14.30	4
U715	13.30	3
U927	14.30	3
U944	14.00	2
U1190	16.50	3
U1225	16.50	3
U1556	14.20	3
U1706	14.70	2
U1837	15.20	4
U1892	15.30	3
U1964	13.40	2

NOTE.—Col. (1): UGC name for galaxy. Col. (2): Observed blue apparent magnitude, m_B , taken from Zwicky et al. (1961–1968) for $m_B < 15.7$; from Nilson (1973) estimate otherwise. See note to Table 9 for comments on col. (3).

evident that more E/S0 galaxies are detected than are spiral/irregular galaxies. Indeed, among the spiral/irregular galaxies, almost all the X-ray-detected galaxies are in the S-A; very few are in the UGC or ESO samples.

Our choice of $S/N = 2.5$ as the dividing line between detected and undetected galaxies in our survey comes from two results evident in these histograms. First, only 4/194

(=2%) of the blank fields have S/N values greater than 2.5. Second, the negative S/N tails of the blank fields and of the spiral/irregular UGC and ESO galaxy samples are well matched, indicating the galaxy observations have a similar intrinsic S/N distribution as the blank fields. Based on the blank field observations, we would estimate that as many as five galaxies with fluxes near the $S/N = 2.5$ cutoff (2% of the detected sample) could have spurious detections.

4.2. Comparison with the Published Data

Fabbiano, Kim, & Trinchieri (1992) have published *Einstein* observations for 405 individual galaxies, all of which are taken from the RC2 catalog. Given the format in which their data are published, we can compare the results of our survey with theirs in two ways: by count rate and by fully corrected X-ray luminosity. For this comparison we find that we should exclude 22 galaxies from F92 that have only HRI observations, as we have used only IPC observations for our samples.

On further comparison, we find only 285 of the remaining 383 galaxies have quoted count rates and luminosities in common between both samples. Of the 98 galaxies that have F92 IPC observations but are not in our sample, almost all were excluded from our sample because of various objective selection criteria (e.g., size, diffuse emission, non-UGC/ESO/S-A, too short an image exposure). Ten galaxies are not in this comparison, as they are among the few UGC galaxies not observed for the present survey.

In 112 of these 285 galaxies in common, both our data and those of F92 are upper limits. Because comparing just the upper limit values for galaxy fluxes is inconclusive, this leaves us with 173 galaxies for which we can make a meaningful comparison with F92. Of these, 137 have detections in both data sets, 25 are detected by us and not by F92, and 11 are detected by F92 and not by us. Our survey has detected 251 galaxies (including those galaxies with and without radial velocities) at the 2.5σ level or higher. Thus, our sample contains 89 X-ray-detected galaxies not previously published in the F92 compilation, a 43% increase over the 207 X-ray-detected galaxies listed by F92.

That we have generally good agreement between our fully corrected X-ray luminosities and those of F92 is shown in Figure 5 for the 137 galaxies detected in common between the two data sets. F92 fluxes have been adjusted to our distances for this comparison. As can be seen from Figure 5, while the relative flux scales between F92 fluxes and ours are the same, there are some differences in zero points. To examine this latter point more closely, Figure 6a shows the logarithm of the ratio of the F92 X-ray fluxes to our fluxes, plotted versus our X-ray fluxes, for galaxies detected by either data sample. The two dotted lines give the median values for $\log [L_X(\text{Us})/L_X(\text{F92})]$ as a function of Hubble type only for the galaxies detected by both surveys: -0.05 for E, S0, and I0 galaxies; -0.12 for spiral galaxies.

Such Hubble type-dependent differences can arise either from differences in energy range observed or in H I-dependent correction for spectral energy distribution differences. To separate these two effects, in Figure 6b we plot the logarithm of the ratio of the observed count rates, $\log [Ct(\text{Us})/Ct(\text{F92})]$ as a function of Hubble type, using the RC3 numerical code for Hubble type (see notes to Table 5). The four galaxies detected in this survey with fluxes and

TABLE 11
ESO GALAXIES WITHOUT X-RAY
OBSERVATIONS

Name (1)	m_B (2)	Omit (3)
E293-G31	15.34	4
E293-G35	16.72	0
E474-G06	14.14	2
E540-G23	14.46	2
E243-G41	14.47	4
E243-G46	12.23	4
E243-G52	14.72	4
E52-G06	15.52	2
E114-G17	17.27	4
E198-IG03	16.45	3
E416-G19	14.61	4
E480-IG08	15.00	2
E547-G03	15.06	3
E31-G09	16.43	2
E357-G18	15.49	3
E83-IG02	17.16	3
E357-G27	14.36	3
E548-G19	14.25	4
E155-IG31	17.01	2

NOTE.—Col. (1): ESO catalog name for galaxy. Col. (2): Observed blue apparent magnitude, m_B , taken from Lauberts & Valentijn (1989). See note to Table 9 for comments on col. (3).

TABLE 12
DERIVED PROPERTIES OF X-RAY-OBSERVED SHAPLEY-AMES GALAXIES

Name (1)	v_{helio} (km s ⁻¹) (2)	Distance (Mpc) (3)	Distance Source (4)	M_B (mag) (5)	log D (kpc) (6)	log L_X (ergs s ⁻¹) (7)	Seyfert (8)
N128	4241	54.81	10	-21.22	1.71	<40.93	...
N221	-205	0.70	98	-15.38	0.22	37.47	...
N227	5305	67.95	1	-21.53	1.62	<40.96	...
SMC	190	0.03	98	-14.51	0.35	<34.37	...
N309	5649	73.32	10	-22.26	1.84	<41.00	...
I1613	-237	0.80	98	-14.54	0.45	<36.96	...
N521	5028	65.31	10	-21.78	1.82	<41.06	...
N520	2059	27.59	10	-20.23	1.57	<40.12	...
N524	2421	32.15	10	-21.20	1.50	40.80	...
N533	5538	64.44	1	-21.69	1.84	42.11	...
N578	1597	26.41	2	-20.92	1.56	<40.16	...
N596	1890	19.81	1	-19.85	1.30	<39.74	...
N598	-204	0.87	98	-18.92	1.21	38.97	...
N613	1510	31.43	2	-21.89	1.72	<40.42	...
N615	1848	29.52	6	-20.73	1.52	<40.21	...
N625	383	4.57	10	-16.10	0.58	<38.74	...
N628	632	9.89	10	-20.40	1.48	39.40	...
N672	390	6.67	10	-18.60	1.11	<38.85	...
N720	1716	27.06	1	-21.04	1.52	40.87	...
N772	2454	36.51	2	-22.21	1.88	<40.82	...
N877	3983	52.71	10	-21.63	1.59	40.96	...
N936	1400	20.13	10	-20.49	1.49	40.17	...

NOTE.—Table 12 is published in its entirety in computer-readable form in the AAS CD-ROM Series, Vol. 9. Col. (1): Galaxy name; N = NGC, I = IC. Col. (2): Heliocentric radial velocity (km s⁻¹), taken from either ZCAT (J. Huchra 1988, private communication) or NED. Col. (3): Quoted distance (Mpc) for the galaxy, assuming $H_0 = 75 \text{ km s}^{-1} \text{ Mpc}^{-1}$. Col. (4): The source of quoted distance. All independent distance measurements come from Willick et al. (1996b); see references therein for details of individual data sets. The abbreviations correspond to the notation of Willick et al. 1 = Faber et al. (1989); 2 = Tormen & Burstein (1995) reanalysis of Aaronson et al. (1982) $H_{-0.05}$ magnitudes (A82); 3 = Han & Mould et al. northern survey data (e.g., Han & Mould 1992; HM); 4 = Han & Mould et al. southern survey data (e.g., Han & Mould 1992; HM); 5 = Courteau and Faber data (CF; Courteau 1992); 6 = Mathewson, Ford, & Buchhorn (1992; MAT); 7, 8 = Willick (Willick et al. 1996b); 9 = from Faber-Burstein Great Attractor velocity field model for an associated cluster or a Local Group galaxy; 10 = from Faber-Burstein Great Attractor velocity field model for this galaxy; 90 = from Mark II data set (Burstein 1989); 99 = from Willick et al. (1996b) but observed two or more times. Col. (5): Absolute blue magnitude corrected for Galactic extinction, K -correction and internal extinction (spirals and irregulars). Col. (6): Absolute log D_{25} diameter, in units of kpc, corrected for Galactic extinction. Col. (7): log L_X , X-ray luminosity (ergs s⁻¹). Col. (8): Active galaxy flag: 1 = Seyfert 1, 2 = Seyfert 2, 3 = Seyfert ?. Seyfert classifications based on NED definitions.

count rates that differ significantly from those of F92 are noted by NGC number. In Figure 6b the dotted lines correspond to the median log ratios of count rates, U_s to F92, of -0.12 for E, S0, and I0 galaxies and -0.10 for S0 and spiral galaxies. To an accuracy of 0.01 dex, our count rates differ from those of F92 by 0.1 dex, in the sense that our count rates are lower.

We thus see that the differences between our fluxes and those of F92 are a combination of differences in observed count rates and differences in conversion of counts to flux. That our observed count rate is systematically lower than that of F92 is to be expected, as we used a different energy range with the IPC than they did: F92 is quoted as using 0.2–4.0 keV; we use 0.5–4.5 keV. Similarly, it is also the case that our final luminosities should differ somewhat from those quoted by F92 as well. F92 used a bremsstrahlung spectrum of 5 keV for the spirals and irregulars and a Raymond spectrum of 1 keV for the ellipticals and S0's. As explained previously (§ 2.2), for our sample we did not a priori distinguish among Hubble types as to the physical source(s) of their X-ray spectra in converting observed count rate to X-ray flux.

Of the four galaxies that show significantly different F92

fluxes than our measurements, NGC 2832, NGC 1399, and NGC 4406 are all elliptical galaxies whose measured X-ray flux can be influenced by emission from diffuse cluster gas. NGC 5850 is a spiral galaxy with relatively low count rate (0.0053 counts s⁻¹). The sense of the difference, $U_s/F92$, is that in the case of the three elliptical galaxies, our measurements do not include any diffuse cluster gas, while in the case of the spiral galaxy, it is likely due to a small difference in how the background was treated.

Given the current uncertainty in the true X-ray energy distributions from galaxies, we accept that differences of ~ 0.1 dex can occur among quoted luminosities derived from the same data under different assumptions. Indeed, we find it comforting that, to a level of 0.1 dex, the X-ray fluxes measured by F92 and by us are consistent with each other. While we find six galaxies (3.5% of galaxies detected by one or the other survey) have significant discrepant fluxes between the two data samples (including two upper limits), this is to be expected. Such differences can occur because of such problematic measurement issues as background flux estimation on the IPC images and possible confusion of cluster diffuse emission with galaxy emission. In both cases, our measurement technique differs enough from that used

TABLE 13
DERIVED PROPERTIES OF X-RAY-OBSERVED UGC GALAXIES

Name (1)	v_{helio} (km s ⁻¹) (2)	Distance (Mpc) (3)	Distance Source (4)	M_B (mag) (5)	log D (kpc) (6)	log L_X (ergs s ⁻¹) (7)	Seyfert (8)
U81	6674	86.19	10	-20.08	1.53	<41.20	...
U144	5620	72.40	10	-19.58	1.30	<40.98	...
U204	5714	70.23	3	-20.09	1.45	<41.01	...
U305	9934	129.12	10	-20.64	1.73	<41.53	...
U387	5296	68.61	10	-20.62	1.64	<41.00	...
U412	5484	71.12	10	-19.04	1.34	<41.05	...
U442	4930	64.00	10	-19.42	1.54	<40.75	...
U446	6263	81.37	10	0.00	1.49	<40.95	...
U499	4719	61.45	10	-19.25	1.49	41.37	2
U509	5136	73.20	7	0.00	1.47	<41.33	...
U524	10781	140.68	10	-21.59	1.59	43.12	1
U573	4980	64.67	10	-20.29	1.44	<41.06	...
U595	13427	175.43	10	-21.75	1.87	<42.02	...
U611	5410	70.13	10	-19.88	1.36	<41.16	...
U626	5856	75.81	10	-19.64	1.36	<41.18	...
U633	5573	72.31	99	-21.00	1.53	<41.34	...
U657	4978	64.91	10	0.00	1.38	<40.74	...
U711	2010	35.07	2	-19.33	1.55	<40.36	...
U712	5215	68.07	10	-20.05	1.40	<40.90	...
U714	4617	63.31	7	-19.99	1.39	<40.96	...
U768	13839	180.92	10	-21.14	1.81	<41.80	...
U784	4902	88.73	5	-20.42	1.61	<40.97	...

NOTE.—Table 13 is published in its entirety in computer-readable form in the AAS CD-ROM Series, Vol. 9. Col. (1): UGC galaxy name. Col. (2): Heliocentric radial velocity (km s⁻¹), taken from either ZCAT (J. Huchra 1988, private communication) or NED. Col. (3): Quoted distance (Mpc) for the galaxy, assuming $H_0 = 75 \text{ km s}^{-1} \text{ Mpc}^{-1}$. Col. (4): The source of quoted distance. All independent distance measurements come from Willick et al. (1996b); see references therein for details of individual data sets. The abbreviations correspond to the notation of Willick et al. 1 = Faber et al. (1989); 2 = Tormen & Burstein (1995) reanalysis of Aaronson et al. (1982) $H_{-0.05}$ magnitudes (A82); 3 = Han & Mould et al. northern survey data (e.g., Han & Mould 1992; HM); 4 = Han & Mould et al. southern survey data (e.g., Han & Mould 1992; HM); 5 = Courteau and Faber data (CF; Courteau 1992); 6 = Mathewson, Ford, & Buchhorn (1992; MAT); 7, 8 = Willick (Willick et al. 1996b); 9 = from Faber-Burstein Great Attractor velocity field model for an associated cluster or a Local Group galaxy; 10 = from Faber-Burstein Great Attractor velocity field model for this galaxy; 90 = from Mark II data set (Burstein 1989); 99 = from Willick et al. (1996b) but observed two or more times. Col. (5): Absolute blue magnitude corrected for Galactic extinction, K -correction and internal extinction (spirals and irregulars). Col. (6): Absolute log D_{25} diameter, in units of kpc, corrected for Galactic extinction. Col. (7): log L_X , X-ray luminosity (ergs s⁻¹). Col. (8): Active galaxy flag: 1 = Seyfert 1, 2 = Seyfert 2, 3 = Seyfert ?. Seyfert classifications based on NED definitions.

by F92 to lead to possible large differences in a few cases.

We believe our method of doing essentially X-ray aperture photometry with the *Einstein* database is complementary to the technique employed by F92. In that paper, following their previous studies, those authors dealt with the IPC and HRI images in an analogous manner as one would do CCD surface photometry of galaxies, including global mapping of the response function. In contrast, our technique is more akin to photoelectric aperture photometry, complete with determining the X-ray “sky background” separately for each object.

Checks also were made of our measurements against earlier compilations (e.g., Forman, Jones, & Tucker 1985; Roberts et al. 1991), and very good consistency was found. However, for these comparisons we note that the same procedures, by a subset of the same authors, were used to derive the fluxes.

5. SUMMARY

We have made an X-ray survey of the *Einstein* IPC images that contain galaxies found in three catalogs—the

Shapley-Ames, the UGC, and the ESO—selected according to well-defined objective criteria. The X-ray fluxes for a total of 1018 galaxies were obtained, 313 in the S-A catalog, 393 non-S-A galaxies in the UGC, and 312 non-S-A ESO galaxies. Our manner of obtaining the X-ray fluxes is analogous to obtaining optical photoelectric measurements: we locate apertures of defined sizes at the optical positions of the galaxies and sample background at symmetric areas of the IPC field. In this way, our analysis differs from that done by Fabbiano et al. (F92), for which the analogy of CCD-like surface photometry is more applicable.

For these galaxies we have assembled associated optical data and have assigned distances according either to direct measurements (Tully-Fisher for spirals and $D_n - \sigma$ for ellipticals) or to the velocity field model of Faber & Burstein (1988).

The accuracy of our X-ray fluxes has been checked in four independent ways. First, we also measured X-ray flux at 194 random IPC positions in the same manner as for our program galaxies. The signal-to-noise histogram of these “blank” fields is reasonably Gaussian in distribution, with

TABLE 14
DERIVED PROPERTIES OF X-RAY-OBSERVED ESO GALAXIES

Name (1)	v_{helio} (km s ⁻¹) (2)	Distance (Mpc) (3)	Distance Source (4)	M_B (mag) (5)	log D (kpc) (6)	log L_X (ergs s ⁻¹) (7)	Seyfert (8)
E349-G31.....	207	3.16	10	-11.96	-0.12	<38.40	...
E349-G37.....	14910	196.00	10	-21.64	1.73	<42.08	...
E474-G05.....	2928	42.75	6	-19.82	1.38	<40.61	...
E540-G19.....	4113	53.91	10	-19.09	1.14	<40.58	...
E540-G24.....	6315	82.47	10	-19.13	1.19	<40.82	...
E540-G25.....	6351	82.95	10	-20.18	1.39	<40.88	...
E244-G01.....	8066	107.15	10	-20.26	1.46	<41.34	...
E113-IG45.....	13834	184.05	10	-22.45	1.62	44.30	1
E114-G16.....	6999	94.79	10	-21.36	1.67	<41.28	...
E298-G07.....	6138	81.71	10	-20.02	1.41	<41.17	...
E298-G16.....	5201	73.08	6	-21.50	1.60	<40.77	...
E479-G20.....	3044	41.52	10	-19.13	1.24	<40.38	...
E479-G21.....	2811	38.41	10	-14.55	0.56	<40.44	...
E416-G25.....	4997	74.13	6	-20.91	1.65	<41.30	...
E416-G28.....	5970	79.73	10	-20.59	1.43	<41.25	...
E416-G29.....	6030	80.53	10	-20.47	1.56	<41.31	...
E416-G31.....	6958	92.64	10	-21.94	1.79	42.49	...
E416-G33.....	6565	70.04	6	-19.47	1.33	<41.08	...
E416-G34.....	7104	94.59	10	-20.39	1.50	<41.40	...
E416-G36.....	7151	95.21	10	-20.88	1.46	<41.38	...
E116-IG07.....	8553	115.51	10	-19.81	1.42	<41.59	...

NOTE.—Table 14 is published in its entirety in computer-readable form in the AAS CD-ROM Series, Vol. 9. Col. (1): ESO catalog name for the galaxy. Col. (2): Heliocentric radial velocity (km s⁻¹), taken from either ZCAT (J. Huchra 1988, private communication) or NED. Col. (3): Quoted distance (Mpc) for the galaxy, assuming $H_0 = 75 \text{ km s}^{-1} \text{ Mpc}^{-1}$. Col. (4): The source of quoted distance. All independent distance measurements come from Willick et al. (1996b); see references therein for details of individual data sets. The abbreviations correspond to the notation of Willick et al. 1 = Faber et al. (1989); 2 = Tormen & Burstein (1995) reanalysis of Aaronson et al. (1982) $H_{-0.05}$ magnitudes (A82); 3 = Han & Mould et al. northern survey data (e.g., Han & Mould 1992; HM); 4 = Han & Mould et al. southern survey data (e.g., Han & Mould 1992; HM); 5 = Courteau and Faber data (CF; Courteau 1992); 6 = Mathewson, Ford, & Buchhorn (1992; MAT); 7, 8 = Willick (Willick et al. 1996b); 9 = from Faber-Burstein Great Attractor velocity field model for an associated cluster or a Local Group galaxy; 10 = from Faber-Burstein Great Attractor velocity field model for this galaxy; 90 = from Mark II data set (Burstein 1989); 99 = from Willick et al. (1996b) but observed two or more times. Col. (5): Absolute blue magnitude corrected for Galactic extinction, K -correction and internal extinction (spirals and irregulars). Col. (6): Absolute log D_{25} diameter, in units of kpc, corrected for Galactic extinction. Col. (7): log L_X , X-ray luminosity (ergs s⁻¹). Col. (8): Active galaxy flag: 1 = Seyfert 1, 2 = Seyfert 2, 3 = Seyfert ?. Seyfert classifications based on NED definitions.

an offset (+0.095) in S/N and only four observations lying beyond the 2.5σ level. Hence, we choose the lower limit for an X-ray detection in this survey to be 2.5σ . Second, X-ray fluxes on 97 IPC images were measured independently by two of us. Third, the negative side of the S/N histogram of the blank fields matches well the negative side of the S/N histogram of the program galaxies with the least intrinsic X-ray flux: the spiral and irregular galaxies.

Fourth, we have made a quantitative comparison with the X-ray fluxes and count rates published by Fabbiano et al. for 173 galaxies in common for which a galaxy was detected in either one or both of the samples. This comparison shows that the published fluxes differ by ± 0.1 dex, owing primarily to differences in the assumptions made for converting observed count rates to flux.

Altogether we have 251 galaxies with detected X-ray flux (at the 2.5σ level or higher), or 24.7% of the sample. Eighty-nine of the detected galaxies are new, not previously cataloged by F92. Based on the S/N distribution of blank fields, as many as five of the detections may be spurious, which yields a true detection rate of 22.6%. The majority of galaxies, 767 in this sample, have only upper limit X-ray

values, a result anticipated at the start of this survey. S/N histograms of the galaxies, divided into broad Hubble type bins of E+S0+I0, S+Irr and by catalog, show the expected result that the S-A galaxies, being the nearest, are detected at a much higher rate than UGC or ESO galaxies. These data will be used in a subsequent paper to revisit issues pertaining to X-ray flux generation in galaxies.

This research was supported by a NASA grant NAG 8-665 and 8-734 and by an ASU faculty grant-in-aid to D. B. A. P. M. was supported by NASA JOVE grant NAG 8-264. The hospitality of the Center for Astrophysics is gratefully acknowledged, as well as the assistance of the *Einstein* data reduction team. This research has made use of the NASA/IPAC Extragalactic Database (NED), which is operated by the Jet Propulsion Laboratory, California Institute of Technology, under contract with the National Aeronautics and Space Administration. C. J. F. and W. R. F. acknowledge support from the Smithsonian Institution and the AXAF Science Center (NASA contract NAS 8-39073).

TABLE 15
OBJECTS FOR WHICH NO REDSHIFT IS KNOWN

Name	Name	Name	Name	Name	Name
X-Ray Detected					
U4924 E482-G15 E347-G09	U10978 E497-G37	U11148 E443-G18	U11172 E444-G70	U11197 E444-G85	E595-G07
X-Ray Upper Limits					
U924	U1015	U1208	U1614	U1619	U1666
U1668	U1731	U2015	U2560	U3648	U3654
U3891	U3921	U4335	U4547	U4577	U5594
U5624	U6125	U6268	U6468	U6808	U6830
U7076	U7077	U7269	U7274	U7411	U7837
U7844	U8250	U8612	U8663	U8761	U8982
U8986	U9039	U9060	U9080	U9129	U9140
U9725	U9848	U10464	U10632	U10895	U10896
U10911	U11106	U11116	U11153	U11228	U11286
U11334	U11412	U11543	U12062	U12324	
E50-G10	E540-G26	E29-G26	E541-G16	E476-G14	E29-G47
E543-G03	E476-G29	E543-G06	E543-G09	E413-G25	E298-G10
E298-G11	E298-G12	E197-G33	E480-G22	E547-G06	E116-IG06
E248-G08	E548-G01	E301-G08	E357-G24	E155-G26	E548-G22
E548-G24	E155-G37	E358-G14	E358-G16	E155-G52	E482-G11
E482-G12	E482-G14	E548-G59	E482-G24	E548-G69	E156-IG07
E482-G40	E549-G53	E550-G01	E156-G40	E55-G11	E303-IG13
E251-G17	E485-G05	E551-G26	E118-G42	E119-G03	E119-G04
E56-G15	E486-G06	E552-G46	E56-G04	E553-G46	E554-G01
E554-G03	E86-G10	E488-G36	E424-G29	E33-G30	E86-G35
E57-G53	E555-G40	E87-G16	E161-IG09	E161-G13	E34-G09
E34-IG10	E162-G03	E492-G07	E560-G05	E561-G27	E495-G17
E90-G16	E436-G04	E375-G28	E503-G01	E266-G09	E320-G16
E266-G13	E266-G18	E440-G16	E572-G43	E572-G45	E441-G01
E505-G24	E322-G39	E506-G26	E322-G41	E506-G37	E322-G62
E576-G25	E508-G56	E508-G57	E324-G14	E324-G19	E444-G31
E444-G73	E444-G88	E132-G16	E445-G11	E445-G29	E578-G20
E272-G01	E448-G09	E395-G04	E396-G11	E397-G13	E397-G15
E339-G02	E399-G16	E595-G16	E595-G17	E73-G31	E73-IG39
E597-G28	E342-IG10	E342-G12	E530-G43	E466-G23	E601-G20
E603-G02	E290-IG43	E407-G04	E291-G15	E471-G35	

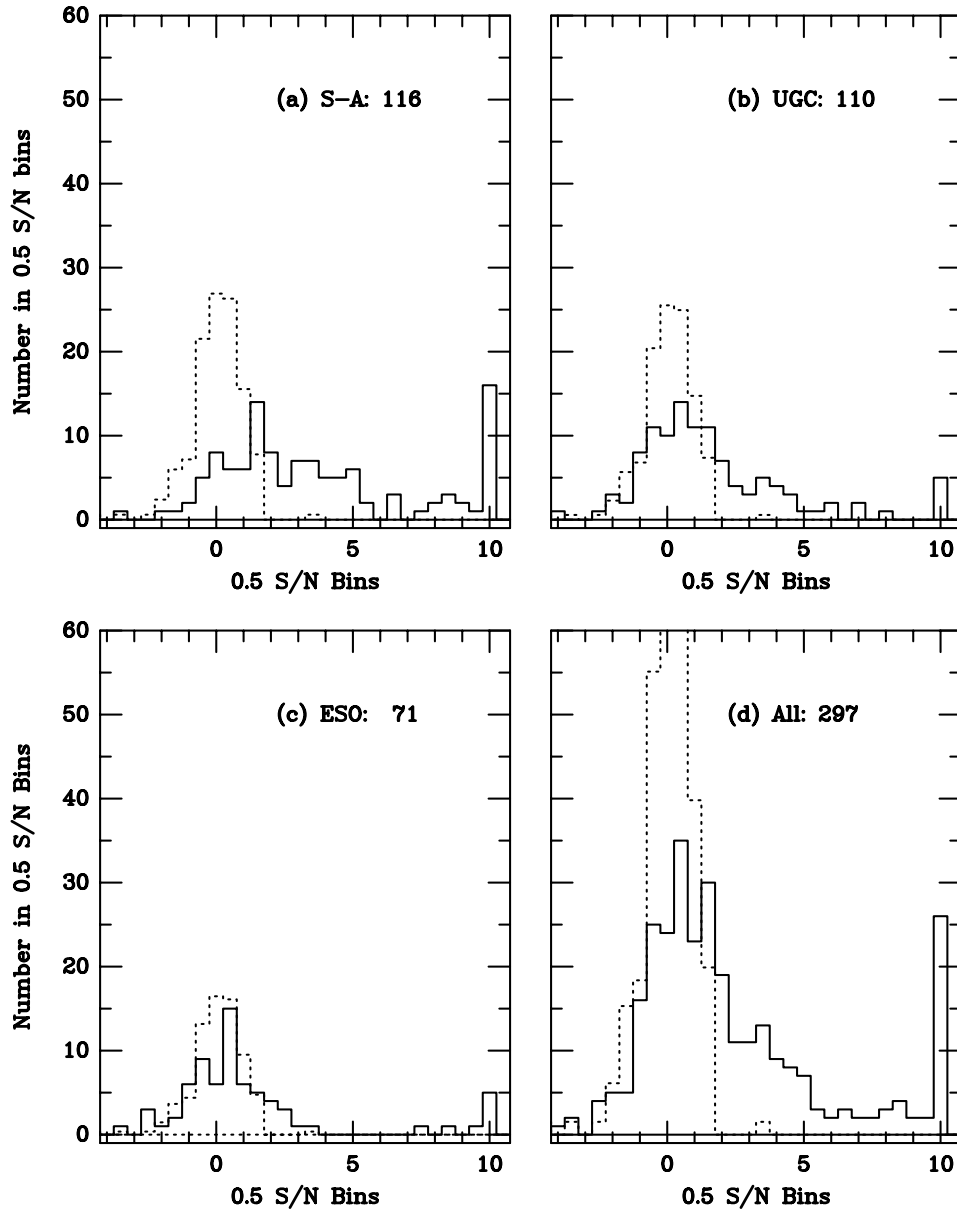


FIG. 3.—(a–d) The IPC S/N distributions for E+S0 galaxies for each of the three optical catalogs (a–c) plus the three catalogs combined (d). In each case, the S/N histogram obtained from the 194 blank fields is overplotted (dotted line). Note the good match of the negative tails of the S/N disruptions of the blank fields and program fields for the UGC and ESO samples.

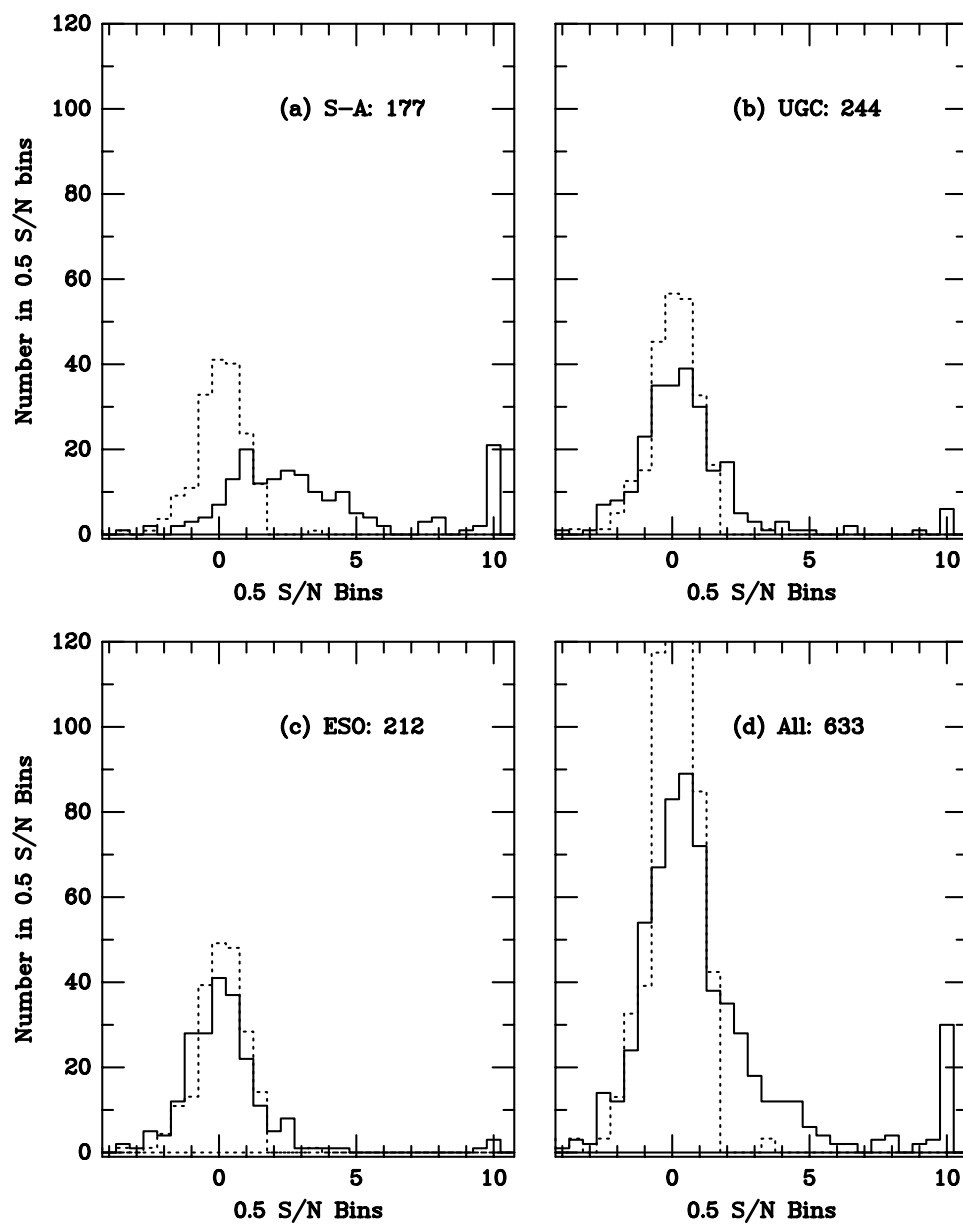


FIG. 4.—Same as Fig. 3, except for different optical catalogs

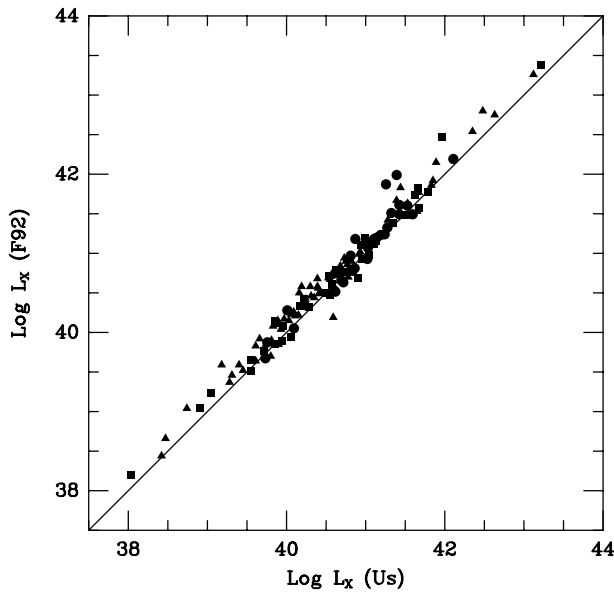


FIG. 5.—F92 X-ray luminosities plotted vs. our X-ray luminosities for 137 galaxies detected in common between our two surveys. Filled circles are X-ray luminosities for E and S0 galaxies, filled squares are early-type spirals, and filled triangles are late-type spirals and irregulars.

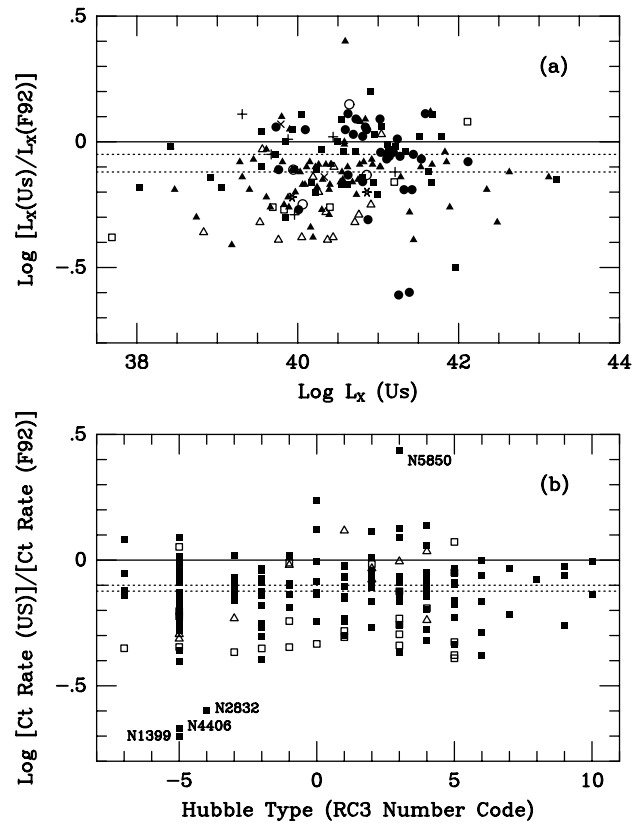


FIG. 6.—(a) The logarithm of the ratio of X-ray luminosity as determined in this survey [$L_X(Us)$] to that determined by F92 [$L_X(F92)$], plotted as a function of $\log L_X(Us)$. Filled symbols are detections in both surveys; open symbols are detections by Us but F92 upper limits; plus signs, crosses, and asterisks are detections by F92 but Us upper limits. Circles and asterisks are E galaxies, squares and plus signs are S0+I0 galaxies, triangles and crosses are spiral and irregular galaxies. The dotted lines mark the median log ratio for E+S0+I0 galaxies (-0.05) and S+I galaxies (-0.12). (b) The logarithm of measured count rates, Us to F92, now plotted as a function of RC3 Hubble type number code. Median values for E+S0+I0 galaxies (-0.12) and for S+I galaxies (-0.10) are shown as dotted lines. Here filled squares are mutual detections, open squares are detections by Us but F92 upper limits, and open triangles are detections by F92 but Us upper limits.

REFERENCES

- Aaronson, M., et al. 1982, *ApJS*, 50, 241
 Burstein, D. 1989, *Mark II Catalog of Galaxy Peculiar Velocities*
 Burstein, D., Haynes, M. P., & Faber, S. M. 1991, *Nature*, 353, 515
 Burstein, D., & Heiles, C. 1984, *ApJS*, 54, 33
 Burstein, D., Willick, J. A., & Courteau, S. 1995, in *Opacity of Spiral Disks*, ed. J. I. Davies & D. Burstein (Dordrecht: Kluwer), 73
 Canizares, C. R., Fabbiano, G., & Trinchieri, G. 1987, *ApJ*, 312, 503
 Courteau, S. 1992, Ph.D. thesis, Univ. California, Santa Cruz
 Davies, J. I., Jones, H., & Trewella, M. 1995, in *Opacity of Spiral Disks*, ed. J. I. Davies & D. Burstein (Dordrecht: Kluwer), 85
 de Vaucouleurs, G., de Vaucouleurs, A., & Corwin, H. G. 1976, *Second Reference Catalogue of Bright Galaxies* (Austin: Univ. Texas Press) (RC2)
 de Vaucouleurs, G., de Vaucouleurs, A., Corwin, H. G., Buta, R. J., Paturel, G., & Fouqué, P. 1991, *Third Reference Catalogue of Bright Galaxies* (New York: Springer) (RC3)
 Dressel, L. L., & Condon, J. J. 1976, *ApJS*, 31, 187
 Fabbiano, G., Kim, D.-W., & Trinchieri, G. 1992, *ApJS*, 80, 531 (F92)
 Fabbiano, G., & Trinchieri, G. 1987, *ApJ*, 315, 46
 Faber, S. M., & Burstein, D. 1988, in *Large-Scale Motions in the Universe*, ed. V. C. Rubin & G. V. Coyne (Princeton: Princeton Univ. Press), 115
 Faber, S. M., Wegner, G., Burstein, D., Davies, R. L., Dressler, A., Lynden-Bell, D., & Terlevich, R. J. 1989, *ApJS*, 69, 763
 Forman, W., Jones, C., & Tucker, W. 1985, *ApJ*, 277, 19
 Giovanelli, R. 1995, in *Opacity of Spiral Disks*, ed. J. I. Davies & D. Burstein (Dordrecht: Kluwer), 127
 Han, M. S., & Mould, J. R. 1992, *ApJ*, 396, 453
 Harris, et al. 1991, *The Einstein IPC Source Catalog* (Cambridge: Smithsonian Astrophys. Obs.)
 Huchra, J. 1976, *AJ*, 81, 952
 Lauberts, A. 1982, *The ESO/Uppsala Survey of the ESO (B) Atlas* (Garching: ESO) (ESO)
 Lauberts, A., & Valentijn, E. A. 1989, *The Surface Photometry Catalogue of the ESO-Uppsala Galaxies* (Garching: ESO)
 Long, K. S., & Van Speybroeck, L. P. 1981, in *Accretion-driven X-Ray Sources*, ed. W. Lewin & E. P. J. van den Heuvel (Cambridge: Cambridge Univ. Press), 117
 Marshall, F. J., & Clark, G. W. 1984, *ApJ*, 287, 633
 Mathewson, D. L., Ford, V. I., & Buchhorn, M. 1992, *ApJS*, 81, 413
 Nilson, P. 1973, *Uppsala General Catalogue of Galaxies*, *Nova Acta R. Soc. Sci. Uppsala*, ser. V: A, Vol. 1
 Roberts, M. S., Hogg, D. E., Bregman, J. N., Forman, W. R., & Jones, C. 1991, *ApJS*, 75, 751
 Sandage, A., & Tammann, G. A. 1981, *A Revised Shapley-Ames Catalogue of Bright Galaxies* (Washington: Carnegie Inst. Washington)
 Shapley, H., & Ames, A. 1932, *Ann. Harvard Coll. Obs.* 88, No. 2 (S-A)
 Stark, A. A., Gammie, F., Wilson, R. W., Bally, J., Linke, R. A., Heiles, C., & Hurwitz, M. 1992, *ApJS*, 79, 77

- Tormen, G., & Burstein, D. 1995, ApJS, 96, 123
Valentijn, E. A. 1990, Nature, 346, 153
Willick, J. A., Courteau, S., Faber, S. M., Burstein, D., & Dekel, A. 1995, ApJ, 446, 12
Willick, J. A., Courteau, S., Faber, S. M., Burstein, D., Dekel, A., & Kolatt, T. 1996a, ApJ, 457, 460
Willick, J. A., et al. 1996b, ApJS, 109, 333
Zwicky, F., Herzog, E., Kowal, C. T., Wild, P., & Karpowicz, M. 1961–1968, Catalogue of Galaxies and Clusters of Galaxies, 6 Vols. (Pasadena: California Inst. Technology)